

Experimental and statistical analysis of surface charge, aggregation and adsorption behaviors of surface-functionalized titanium dioxide nanoparticles in aquatic system

Chengcheng Xiang · Feng Yang · Ming Li ·
Majid Jaridi · Nianqiang Wu

Received: 23 May 2012 / Accepted: 7 November 2012 / Published online: 13 December 2012
© Springer Science+Business Media Dordrecht 2012

Abstract One hundred and fifty nanometers sized anatase titanium dioxide nanoparticles (TiO₂ NPs) have been functionalized with the -CH₃, -NH₂, -SH, -OH, -COOH, and -SO₃H terminal groups. Surface charge, aggregation, and adsorption behaviors of the functionalized NPs in aquatic phase have been investigated by a set of experiments following the full factorial design. The dependence of surface charge, suspension size, and surface adsorption upon the various factors (including surface chemistry of NPs, the pH value, and ionic strength of an aqueous solution) has been studied with the statistical methods such as multiple linear regressions and multiple comparison tests. The surface functional group on the TiO₂ NPs affects the characteristics in the simulated aquatic environment. The correlations among the characteristics of NPs have also been investigated by

obtaining Pearson's correlation coefficient. The hydrodynamic size is negatively correlated with the absolute value of zeta potential, and positively correlated with the ionic strength. In the NaCl solution, the charge screening effect is responsible for the aggregation. In the CaCl₂ solution, the charge screening effect is dominant mechanism for aggregation at a low salt concentration. In contrast, the interaction between Ca²⁺ ions and the specific functional group plays a significant role at a high salt concentration. The adsorption efficiency of humic acid decreases with an increase in the pH value, whereas increases with an increase in the ionic strength. The adsorption efficiency is positively correlated with the zeta potential. The statistical analysis methods and the results have implications in assessment of potential environmental risks posed by engineered nanoparticles.

Electronic supplementary material The online version of this article (doi:10.1007/s11051-012-1293-7) contains supplementary material, which is available to authorized users.

C. Xiang · M. Li · N. Wu (✉)
Department of Mechanical and Aerospace Engineering,
WVNano Initiative, West Virginia University,
Morgantown, WV 26506-6106, USA
e-mail: nick.wu@mail.wvu.edu

C. Xiang · F. Yang (✉) · M. Jaridi
Department of Industrial and Management Systems
Engineering, West Virginia University, Morgantown,
WV 26506-6107, USA
e-mail: feng.yang@mail.wvu.edu

Keywords Surface chemistry · TiO₂ nanoparticles · Aggregation · Adsorption · Statistical analysis · Experimental design

Introduction

Nanomaterials with at least one dimension less than 100 nm exhibit unique properties different from bulk counterparts (Duan et al. 2001; Li et al. 2011; Tan et al. 2003; Wu et al. 2005; Zhang et al. 2010). With rapid development of nanotechnology, engineered nanomaterials are finding increasing applications in

consumer products and additives. For example, titanium dioxide nanoparticles (TiO₂ NPs) are extensively used for photocatalysis, energy conversion/storage, and biosensing (Li et al. 2008a, b, c; Tafen et al. 2009; Wang et al. 2009, 2010; Wu et al. 2010; Yang et al. 2008). Growing production and use of nanomaterials inevitably increases their release and exposure into the surrounding environment, which raises serious concern on its potential environmental risks and toxicity (Hamilton et al. 2009; Lee et al. 2007; Magrez et al. 2009; Sharma 2009). The environmental concentration of TiO₂ NPs was estimated to be 0.7–16 µg/L. This was close to or higher than a threshold toxicity value of 1 µg/L determined by a recent report (Mueller and Nowack 2008). In natural water, the physicochemical characteristics of NPs change under various environmental conditions (Yang et al. 2009; Domingos et al. 2009; Epling and Lin 2002; French et al. 2009; Solovitch et al. 2010). These alterations will consequently have profound influence on their environmental contamination and toxicity potency. Therefore, to assess the environmental risk and toxicity of TiO₂ NPs, it is essential to quantify the dependence of characteristics of TiO₂ NPs upon the environmental factors in an aquatic system (Zhang et al. 2009).

The water quality parameters, including pH, ionic strength, cation type, and natural organic matters (NOMs) affect the physicochemical characteristics of engineered nanomaterials (Hyung et al. 2007; Hyung and Kim 2008; Smith et al. 2009; Wang et al. 2008). Several investigations have been conducted to examine the effects of the water quality parameters on the aggregation and adsorption behaviors of nanomaterials (Chen et al. 2012; Liu et al. 2011; Keller et al. 2010). It has been found that the NOM adsorption on the carbon nanotubes is strongly dependent on the hydrophobic interaction, π - π interaction, hydrogen bond, electrostatic interaction, and the Van der Waals interaction between adsorbates and engineered nanomaterials (Hyung and Kim 2008). In addition, the uptake and toxicity of gold nanoparticles are dictated by the surface functional group (Zhu et al. 2010). The hydrophilic particles can be ingested and rapidly cleared without obvious health impact, whereas hydrophobic particles are accumulated in the organism with toxic effects. So far, *limited information is available regarding* the effect of surface chemistry on the surface charge and aggregation of

NPs, as well as on the surface adsorption on NPs in aquatic systems.

The objective of this study is threefold: (i) to systematically investigate how the surface charge, aggregation, and surface adsorption behavior of functionalized NPs are affected by a range of factors including functional group (surface chemistry) of the NPs, the pH value and cation type/concentration in an aquatic environment; (ii) to determine the correlation between the hydrodynamic size and the zeta potential, and (iii) to determine the correlation between adsorption efficiency and the zeta potential. Statistical methods are adapted to perform such an investigation. First, full factorial design is used to specify factor combinations (i.e., experimental settings) at which laboratory experiments are carried out (Montgomery 2012). Second, based on the experimental data, multiple linear regression is performed, which evaluates not only the individual factor effects but also the interacting effects of multiple factors in a statistically valid manner (Tamhane and Dunlop 2000). This is in distinct contrast to the conventional one-factor-at-a-time approach which studies the effect of one-factor-at-a-time and is thus not able to examine the interacting effects of factors. Third, the correlation in objectives (ii) and (iii) is estimated by the Pearson method (Tamhane and Dunlop 2000), and statistical significance of such a correlation is evaluated.

Materials and methods

Experimental controllable factors and levels

In our experiments, three controllable factors and the experimental levels for each factor are given in Table 1. The functional group of the NPs, denoted as x_1 , is varied among seven different settings: pristine TiO₂ NPs, NH₂-, SO₃H-, COOH-, OH-, SH-, and CH₃-terminated TiO₂ NPs (Palma et al. 2007; Cano-Serrano et al. 2003). The factor x_2 represents the pH value of the aqueous solution; it is set at three levels, 5, 7, and 9, since the pH value in an aquatic environment is generally in the range of 5–9. For x_3 , the salt condition in the aqueous solution, there are five experimental levels: solution without addition of NaCl/CaCl₂, with 0.01 M NaCl, 0.1 M NaCl, 0.01 M CaCl₂, and 0.1 M CaCl₂. The factor levels of salt condition are specified in this way because the

Table 1 Controllable factors and their experimental levels

Factor	Factor levels
x_1 : Functional group of the NPs	Pristine, $-\text{NH}_2$, $-\text{SO}_3\text{H}$, $-\text{COOH}$, $-\text{OH}$, $-\text{SH}$, and $-\text{CH}_3$
x_2 : pH value	5, 7, 9
x_3 : Cation type and concentration	($[\text{NaCl}] = 0$, $[\text{CaCl}_2] = 0$), ($[\text{NaCl}] = 0.01 \text{ M}$, $[\text{CaCl}_2] = 0$), ($[\text{NaCl}] = 0.1 \text{ M}$, $[\text{CaCl}_2] = 0$), ($[\text{NaCl}] = 0$, $[\text{CaCl}_2] = 0.01 \text{ M}$), ($[\text{NaCl}] = 0$, $[\text{CaCl}_2] = 0.1 \text{ M}$)

ionic strength is 0–0.1 M order of magnitude in surface waters (Epling and Lin 2002), and NaCl and CaCl_2 are the typical cations in soft water and hard water. At a selected factor combination, the TiO_2 NPs were exposed to the liquid solution, and their characteristic responses were measured which include (i) zeta potential $y^{(1)}$, (ii) hydrodynamic size $y^{(2)}$, and (iii) adsorption efficiency $y^{(3)}$ of TiO_2 NPs.

Surface modification of TiO_2 nanoparticles

Engineered TiO_2 NPs with NH_2 , SO_3H , COOH , OH , SH , and CH_3 terminal groups were prepared by surface modification of commercially available TiO_2 using *N*-butyltrimethoxysilane (BTMS), (3-mercaptopropyl) trimethoxysilane (MPTS), (3-glycidoxypropyl) trimethoxysilane (GPTMS), triethoxysilylpropyl succinic anhydride (TESPSA), and 3-aminopropyltriethoxysilane (APTMS), respectively (Palma et al. 2007). Typically, 1.0 g of dry TiO_2 NPs, which were 150 nm sized round-shaped anatase spheres, were first immersed into 10 mL of deionized water, of which pH value was adjusted to 11 by tetramethylammonium hydroxide pentahydrate (5 wt%, TMAOH, $(\text{CH}_3)_4\text{N}-\text{OH}\cdot 5\text{H}_2\text{O}$), to facilitate the adsorption of hydroxyl group. The hydroxyl group rich TiO_2 NPs were washed twice with 20 mL of methanol to remove the excessive TMAOH. The TMAOH-treated TiO_2 NPs were dried in a vacuum oven at room temperature for use. After that, 3 mL of silane coupling agents were added into the TiO_2 suspension in 20 mL of toluene. The suspension was further refluxed at 110 °C for 24 h under an argon flow and vigorous stirring, washed three times with methanol to remove the unreacted silane coupling agents, and then dried in a vacuum oven prior to use.

The $\text{SO}_3\text{H}-\text{TiO}_2$ NPs were prepared by the oxidation of $\text{SH}-\text{TiO}_2$ NPs using H_2O_2 according to a well-established procedure (Cano-Serrano et al. 2003).

Testing of surface charge, aggregation, and adsorption of nanoparticles

Surface charge and aggregation measurements

Five milligrams of modified TiO_2 NPs were dispersed into 500 mL of D.I. water followed by ultrasonication for 10 min to obtain the 10 mg/L TiO_2 stock suspension. Three bottles were put by 100 mL of the prepared TiO_2 suspension, and then the pH value was adjusted to 5, 7, and 9 by addition of 1 M HCl or 1 M NaOH aqueous solution, respectively. Aliquots (~20 mL) of the resulting suspensions were taken out, and the salt concentration was adjusted to 0, 0.01, and 0.1 M by addition of 5 M NaCl or CaCl_2 . Finally, there was a 0.2 U shift in the pH value in both NaCl and CaCl_2 samples because no buffer solution was used.

Adsorption experiments

All adsorption experiments were performed at room temperature. 20 mg of humic acid was added to three vials containing 40 mL of D.I. water, respectively, and then the pH value was adjusted to 5, 7, and 9 by addition of 1 M HCl or NaOH aqueous solution. As a result, the humic acid stock solutions with the concentration of 500 mg/L and pH value of 5, 7, and 9 were obtained, respectively. 200 μL of humic acid stock solution was added to 10 mL of modified TiO_2 suspensions with the same pH value, and then the salt concentration was adjusted to 0, 0.01, and 0.1 M by addition of 5 M NaCl or 5 M CaCl_2 . The resulting suspensions were shaken for 24 h to reach the sorption equilibration for humic acid. After that, the suspensions were centrifuged, and the supernatant was taken out and subjected to the UV–Vis absorption measurement.

Statistical methods

Design of experiments

A full factorial design was adopted for our experiments, and it allowed for the evaluation of the main effect of each factor and the two-factor interaction effects. With the three controllable factors and their experimental levels in Table 1, a total of $105 = 7 \times 3 \times 5$ (7 levels for x_1 , 3 levels for x_2 , and 5 levels for x_3) distinct factor settings were explored following the full factorial design. To reduce the effects of unknown nuisance factors (factors other than the three considered as of interest), the 105 experiments were performed at the 105 factor settings in a completely random order. At each factor setting, one replication was conducted, and the responses of interest were measured.

Multiple linear regressions

To quantify the relationship between the three factors and the responses of TiO₂ NPs, multiple linear regressions were performed to approximate each response, $y^{(i)}$ ($i = 1, 2, 3$) as a function of the factors x_1 , x_2 , and x_3 . Such a model investigates the main factor effects and the two-factor interaction effects. In our regression analysis, all the factors were considered as categorical (nominal) factors, and for each one, several dummy variables were used to represent its experimental levels. To achieve the simplest adequate model, stepwise regression method was adopted in search of the best model describing the x - y relationship. The details of the multiple linear regressions performed in this study are given in Section S1.1 (See the Supplementary material).

Other statistical methods

Following up the linear regressions, multiple comparison tests were carried out to perform pairwise comparison of the effects that various factor levels may have on the response. Consider for example the salt condition factor which has five experimental levels (Table 1). Does the addition of 0.01 M CaCl₂ to the liquid solution have a bigger impact on the responses than the addition of 0.01 M NaCl? In this

study, such questions are addressed by the Tukey–Kramer multiple comparison test in a statistically valid manner (Tamhane and Dunlop 2000).

To investigate the dependence of hydrodynamic size $y^{(2)}$ and adsorption efficiency $y^{(3)}$ upon zeta potential $y^{(1)}$, two-tailed Pearson method was used to evaluate the correlations for $(y^{(1)}, y^{(2)})$ and $(y^{(1)}, y^{(3)})$ pairs, respectively.

Results and discussion

In this part, we present the findings from the experimental data-based statistical modeling and analysis, and explore the causes behind these findings. Three types of statistical methods were used in our work: multiple linear regressions, multiple comparison tests, and Pearson's correlation, which are detailed in Section S1 (See the Supplementary material).

Since a lot of the discussions in this section are based on the regression models (M1, M2, and M3) (See the Supplementary material), those models are briefly explained as follows for the reader's convenience. Take model M1 as an example, which quantifies the response $y^{(1)}$, zeta potential as a function of the selected important dummy variables (D_i ; $i = 1, 2, \dots, 12$). All the variables (D_i ; $i = 1, 2, \dots, 12$) are dichotomous, and takes values of either 1 or 0. In model M1, the content in the parenthesis explains what factor level (e.g., pH 5 in the environment) is associated with D_i ($i = 1, 2, \dots, 12$); all the factor levels are given in Table 1. If a factor level is used in the experiment, then its corresponding dummy variable is set as 1; otherwise it is 0. For instance, for an experiment performed on COOH–TiO₂ NPs in a liquid solution with pH 5 and 0.01 M NaCl, we have: $D_3 = 1$, $D_8 = 1$, $D_{12} = 1$, and the rest of dummy variables are all zero; the expected zeta potential can be estimated by plugging the dummy values into model M1. The case for which all the dummy variables are zero corresponds to the control experiments where pristine NPs are exposed to solution with pH 7 and no salt. Models M2 and M3 can be explained in the same way as M1 for the other two responses, hydrodynamic size $y^{(2)}$, and adsorption efficiency $y^{(3)}$, respectively.

Surface charge and zeta potential

Effect of the pH value on the surface charge

Figure 1a–c plots the zeta potential against pH value for the aqueous solutions with 0, 0.01, and 0.1 M CaCl₂, respectively. First, the zeta potential of nanomaterials generally decreased with an increase in the pH value of the aqueous solution, which was confirmed by our analysis. In model M1, the estimated coefficient for variable $D_8(\text{pH5})$ was 29.7 mV, which indicated a general increase in the zeta potential when the pH value decreased from 7 to 5. At a low pH regime, the surface functional groups on the NPs were substantially protonated and their charge was positive. As the pH value increased, more surface functional groups were dissociated to the negative groups (Ofir et al. 2007; Gu et al. 2009), and more OH⁻ were adsorbed onto the pristine TiO₂ NPs (Fumiaki et al. 2010). Hence, the zeta potential of all types of NPs became more negative as the pH increased. In addition, no term related to $D_7(\text{pH9})$ appeared in the model, which suggested that there was no substantial change in the zeta potential when the pH value increased from 7 to 9. In this pH regime, the surface functional groups were stable.

Second, the surface functional group of nanomaterials affected the dependence of the zeta potential on the pH value (Fig. 1). This was reflected in model M1 by the significant interacting terms between functional groups and pH levels: $D_2(\text{SO}_3\text{H}) \times D_8(\text{pH5})$, $D_3(\text{COOH}) \times D_8(\text{pH5})$, $D_4(\text{COOH}) \times D_8(\text{pH5})$, $D_5(\text{SH}) \times D_8(\text{pH5})$.

Third, with different salt conditions, the zeta potential versus pH trend also changed. This was reflected in model M1 by the significant interacting terms between pH and salt conditions: $D_8(\text{pH5}) \times D_9(0.1 \text{ CaCl}_2)$, $D_8(\text{pH5}) \times D_{10}(0.01 \text{ CaCl}_2)$, $D_8(\text{pH5}) \times D_{11}(0.1 \text{ NaCl})$, $D_2(\text{SO}_3\text{H}) \times D_{12}(0.01 \text{ NaCl})$. This is illustrated by the sequence of graphs in Fig. 1. In Fig. 1a, b where [CaCl₂] was 0 and 0.01 M (low), the zeta potential typically decreases with increasing the pH value. But when [CaCl₂] was 0.1 M (high), the increasing pattern dominates as shown in Fig. 1c. This was because at high [CaCl₂], the dissociated surface groups (as a result of high pH value) can bind to the Ca²⁺ through the bridge binding (Kim et al. 2001).

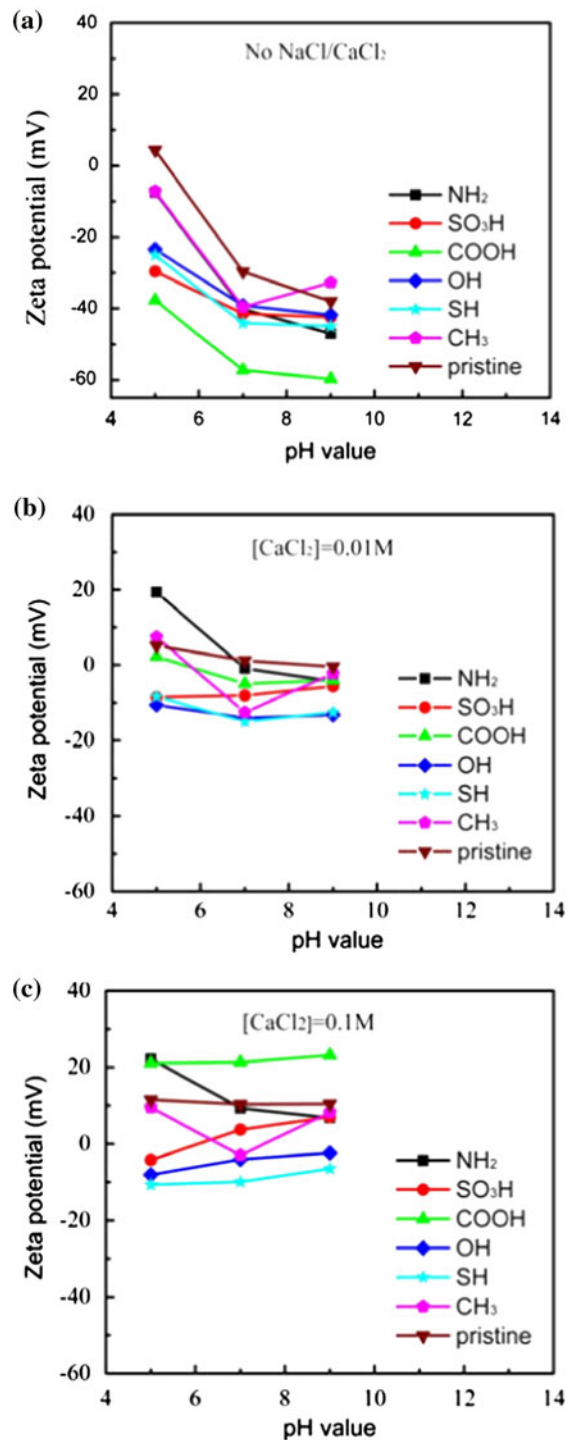


Fig. 1 Zeta potential of various surface-functionalized TiO₂ nanoparticles as a function of the pH value at **a** [CaCl₂] = 0 M, **b** [CaCl₂] = 0.01 M and **c** [CaCl₂] = 0.1 M

Effect of the ionic strength on the surface charge

The zeta potential of TiO₂ NPs as a function of the CaCl₂ concentration is shown in Fig. S1 in Supplementary material. The zeta potential of the TiO₂ NPs increased with an increase in the salt concentration, which was mainly due to the fact that the addition of salt increased the ionic strength and reduced the thickness of the electric double layer. This was supported by model M1 in which all the four salt condition levels had significant positive main effects: 41.1 for $D_9(0.1\text{CaCl}_2)$, 31.0 for $D_{10}(0.01\text{CaCl}_2)$, 17.8 for $D_{11}(0.1\text{NaCl})$, and 7.1 for $D_{12}(0.01\text{NaCl})$. For both CaCl₂ and NaCl, a steep increase in zeta potential was obtained when the salt concentration increased from 0 to 0.01 M, while over the concentration range (0.01, 0.1) M, the zeta potential increased much slower with the salt concentration.

Model M1 indicates that COOH is a special functional group since it has a strong positive interaction with CaCl₂: the coefficients of $D_3(\text{COOH}) \times D_9(0.1\text{CaCl}_2)$ and $D_3(\text{COOH}) \times D_{10}(0.01\text{CaCl}_2)$ are positive. This can be graphically explained by Fig. S1. For COOH–TiO₂ NPs, the zeta potential was particularly sensitive to the change in the CaCl₂ concentration. This was due to the fact that Ca²⁺ can chemically bind to the COOH group by the bridge binding in addition to the electrostatic interaction, leading to the faster increase of the zeta potential in comparison with the other TiO₂ NPs (Epling and Lin 2002; Kim et al. 2001). In short, the bridge binding is responsible for the significant two-factor interactions between the COOH group and the CaCl₂ solution from the statistical result. Therefore, the zeta potential of TiO₂ NPs with different functional groups showed the distinct dependence on the salt concentration.

Effect of the cation type on the surface charge

At the same concentration level, CaCl₂ has a higher positive effect on the zeta potential than NaCl. Table S3 provides the Tukey–Kramer comparison results (See the Supplementary material), and shows that the effect difference between CaCl₂ and NaCl varied between (18.7, 30.0) at the level of 0.01 M, and the effect difference ranges among (19.6, 30.9) at 0.1 M. The detailed Tukey–Kramer comparison results are given and discussed in Section S1.2 (See the Supplementary material).

The zeta potentials of all functionalized NPs in the CaCl₂ solution were higher than that in the NaCl, which can be explained by three reasons. First, the addition of divalent Ca²⁺ leads to the higher ionic strength because the ionic strength is positively proportional to not only the concentration of ions but also the chemical valence, expressed by (Li et al. 2009).

$$I = \frac{1}{2} \sum_{i=1}^n C_i Z_i^2. \quad (1)$$

Second, divalent Ca²⁺ results in smaller Debye length ($1/\kappa$) than the monovalent Na⁺. It is well known that the Debye length is the inverse of the Debye parameter (κ) that is expressed as (Epling and Lin 2002; Kim et al. 2001)

$$\kappa = \sqrt{\frac{e^2 \sum n_i Z_i^2}{\epsilon_r \epsilon_0 k_B T}} \quad (2)$$

where e is the electron charge, n_i is the number of ion i in the bulk solution, and z_i is the valence of ion i . Thus decreasing Debye length increases the apparent zeta potential. Third, Ca²⁺ can be adsorbed on the negatively charged NPs by the bridging interaction in some cases in addition to the electrostatic adsorption (Epling and Lin 2002; Kim et al. 2001). Therefore, the zeta potential increases rapidly as the CaCl₂ concentration increases.

In short, the zeta potentials of all types of NPs decreased with an increase in the pH value at a low salt concentration. At a high salt concentration, the zeta potentials of SO₃H[−], COOH[−], OH[−], and SH–TiO₂ NPs slightly increased when pH increased. The zeta potential of COOH–TiO₂ NPs was most sensitive to the CaCl₂ concentration. The effects of charge screening and the functional group will be discussed in more detail later.

Hydrodynamic size in aquatic phase

The particle size measured with the dynamic light scattering (DLS) technique is the hydrodynamic size that reflects the degree of aggregation of particles in the solution, which is different from that observed with TEM and SEM under the dry condition. In general, the existing form of particles in aquatic environment depends on the Van der Waals force, the electrostatic interaction, the hydrogen bonds, the chemical bonds,

etc. The theory of Derjaguin, Landau, Verwey, and Overbeek (DLVO) (Derjaguin et al. 1941; Verwey and Overbeek 1948), which incorporates the Van der Waals force with the electrostatic interaction originated from the presence of electric double layer, has been used for interpreting the stability of colloidal suspensions. According to the DLVO theory, the hydrodynamic size of the charged particle suspensions increases as the ionic strength increases or the surface charge (absolute value of zeta potential) decreases.

Effect of the pH value on the hydrodynamic size

In model M2, no pH related main effects are significant, i.e., neither $D_8(\text{pH}5)$ nor $D_7(\text{pH}9)$ appears in the model. This suggests that pH value does not have a statistically significant main effect on the hydrodynamic size of TiO_2 NPs. In other words, the pH value has no significant effect on the hydrodynamic size in the absence of salts, which can also be confirmed in Fig. S2a in Supplementary material. There are, however, three significant interaction terms related to the pH value in model M2: $-342 \text{ nm } D_8(\text{pH}5) \times D_9(0.1 \text{ CaCl}_2)$, $347 \text{ nm } D_8(\text{pH}5) \times D_{12}(0.01 \text{ NaCl})$, and $-549 \text{ nm } D_1(\text{NH}_2) \times D_8(\text{pH}5)$.

According to the DLVO theory, the hydrodynamic size of particles in the solution strongly depends on both the surface charge and the ionic strength. When the pH value increased in the presence of CaCl_2 , there was no evident change in the zeta potential of NPs except for the $\text{NH}_2\text{-TiO}_2$ NPs (Fig. 1b, c). Consistently, there was no evident change in the hydrodynamic size of NPs except for the $\text{NH}_2\text{-TiO}_2$ NPs (Fig. S2b, c). The zeta potential of the $\text{NH}_2\text{-TiO}_2$ NPs was reduced with an increase in the pH value (Fig. 1b, c), which increased the hydrodynamic size of the $\text{NH}_2\text{-TiO}_2$ NPs (Fig. S2b, c). This suggested that the DLVO mechanism accounted for the aggregation of the NPs in the presence of CaCl_2 .

When the pH value increased in the absence of CaCl_2 , the zeta potential of NPs was reduced (Fig. 1a). However, there was no significant change in the hydrodynamic size of NPs (Fig. S2a).

Effect of the ionic strength on the hydrodynamic size

Figure 2 shows the effect of the CaCl_2 concentration on the hydrodynamic size. Model M2 involves

positive coefficients 602, 568, and 589 nm for $D_9(0.1 \text{ CaCl}_2)$, $D_{10}(0.01 \text{ CaCl}_2)$, and $D_{11}(0.1 \text{ NaCl})$, respectively, indicating that changing the solution from no salt to any one of those three salt conditions will result in substantial increase in the hydrodynamic size of the NPs. The Debye length is inversely proportional to the square root of the ionic strength, and is characteristic of the thickness of double layer. Thus, the thickness of double layer is reduced with the increasing ionic strength (that is, the ion concentration or/and the valence of the cations).

For the NPs with different functional groups, the way that salt concentration affects hydrodynamic size may be different. This is evident from model M2 in which significant interaction effects, 1017 and 1067 nm, are obtained for $D_1(\text{NH}_2) \times D_9(0.1 \text{ CaCl}_2)$ and $D_3(\text{COOH}) \times D_9(0.1 \text{ CaCl}_2)$, respectively. This suggests that for the $\text{NH}_2\text{-TiO}_2$ and the COOH-TiO_2 NPs, the hydrodynamic size increases particularly fast as the CaCl_2 concentration increases in comparison with other NPs, as seen from Figs. 2 and S2c. Generally, the thickness of electrical double layer decreases with an increase in the isoelectric point (Morrison and Ross 2002). The $\text{NH}_2\text{-TiO}_2$ NPs have a very high isoelectric point, thus a very thin electrical double layer, and are more significantly dependent on the ionic strength. On the other hand, it is well known that the amine and the carboxylic groups strongly tend to form the chelate complexes with the metal ions like Ca^{2+} . Such strong chelating bonds can aggravate the aggregation of NPs. Therefore, it is not surprising that the $\text{NH}_2\text{-TiO}_2$ and the COOH-TiO_2 NPs have larger hydrodynamic size than the other NPs at the same CaCl_2 concentration and pH value.

Effect of the cation type on the hydrodynamic size

In the case of low concentration (0.01 M) of salt, addition of 0.01 M CaCl_2 had an estimated main effect of 568 nm on the hydrodynamic size according to model M2, while addition of 0.01 M NaCl had no significant effect. As given in Table S3, the Tukey-Kramer comparison showed that the effect difference between 0.01 M CaCl_2 and 0.01 M NaCl was 404 nm, and could vary over the range of (199, 610 nm). This is due to two mechanisms. First, there is a bridge binding between functional groups and Ca^{2+} while there is no such a binding with Na^+ . Second, Ca^{2+} has higher valence than Na^+ , leading to higher ionic strength.

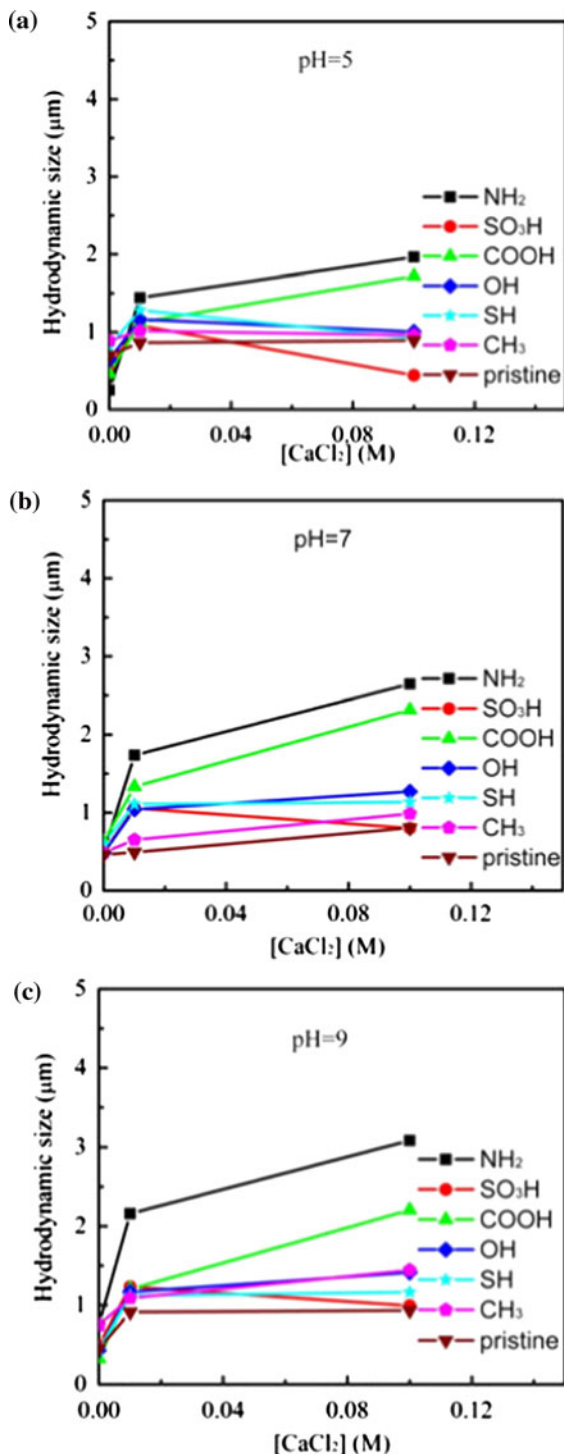


Fig. 2 Hydrodynamic size of various surface-functionalized TiO₂ nanoparticles as a function of the CaCl₂ concentration at a pH 5, b pH 7, and c pH 9

Consequently, the thickness of the electric double layer surrounding the NPs in the CaCl₂ solution is smaller, leading to smaller electrostatic repulsion force. As a result, the hydrodynamic size in CaCl₂ solution is larger. At a low salt concentration (0.01 M), the first mechanism (the charge screening effect) is dominant. Therefore, addition of 0.01 M CaCl₂ had a significant effect. At a high salt concentration (0.1 M), the second mechanism (interaction between Ca²⁺ ions and functional group) is dominant, and 0.1 M salts make the saturated status of the ionic strength level. There is no significant difference in the electrostatic repulsion force induced by CaCl₂ and NaCl. As a result, CaCl₂ and NaCl have comparable effects on the hydrodynamic sizes with the estimated main effects being 602 and 589 nm, respectively, as seen in model M2. The Tukey–Kramer comparison also confirms that there is no significant difference between the effects of 0.1 M CaCl₂ and 0.1 M NaCl (Table S3).

Correlation of the hydrodynamic size with the surface charge

According to the DLVO theory, increasing the surface charge (the absolute value of zeta potential) suppresses the aggregation of NPs, leading to a decrease in the hydrodynamic size. This implies a potential negative correlation between the zeta potential and the hydrodynamic size, which is confirmed in our analysis. Based on the experimental data, the Pearson's correlation between the hydrodynamic size and the absolute value of zeta potential is calculated as -0.409 (Table S4). The negative correlation between the hydrodynamic size and the absolute value of zeta potential is shown in Fig. 3 for the TiO₂ NPs functionalized with various groups, and the statistic parameter describing the correlation can be found in Table S5. This concludes that the DLVO mechanism plays a significant role in the aggregation of the NPs. The NH₂- and COOH-terminated NPs show deviation from this correlation. This is due to the fact that the aggregation/dispersion of these NPs is controlled by additional driving forces (e.g., chelating binding and hydrogen bond) besides the DLVO mechanism.

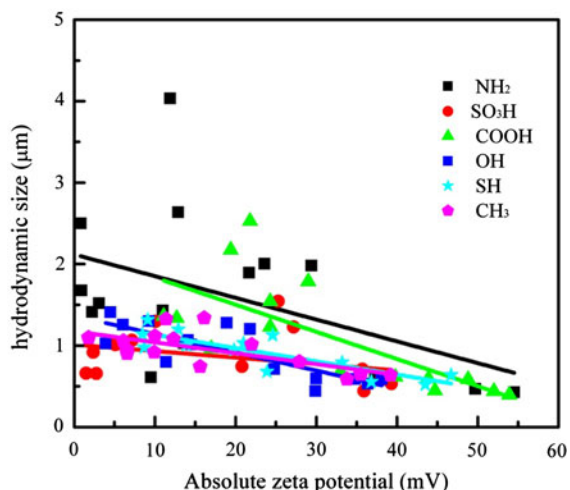


Fig. 3 Correlation of the zeta potential with the hydrodynamic size of various surface-functionalized TiO₂ nanoparticles

Adsorption of humic acid on the TiO₂ particle surface

Humic acid is a common NOM in the wide surface waters. The adsorption of humic acid can change the surface property and thus the behaviors of TiO₂ NPs in the simulated aquatic environment.

Effect of the pH value on the adsorption efficiency

Model M3 suggested that the adsorption of humic acid increased slightly with a decrease in the pH value. More specifically, in model M3, D_8 (pH5) had a small but significant coefficient, indicating that the adsorption efficiency increased when the pH was reduced from 7 to 5. No term related to D_7 (pH9) appeared in model M3, indicating that the adsorption efficiency was little affected when the pH changed from 7 to 9. These trends are graphically illustrated in Fig. S3 in Supplementary material.

As shown above, increasing the pH value led to more adsorption of OH⁻ on the pristine TiO₂ NPs or more negatively charged functional groups on the TiO₂ NPs. It is well known that humic acid is negatively charged. Therefore, increasing the pH enhanced the electrostatic repulsion between the negatively charged NPs and humic acid. As a result, adsorption of humic acid on all types of TiO₂ NPs was reduced with an increase in the pH value.

Effect of the ionic strength on the adsorption efficiency

In model M3, the main effects of all the salt condition levels were significant: 70.5 % for D_9 (0.1 CaCl₂), 67.3 % for D_{10} (0.01 CaCl₂), 20.2 % for D_{11} (0.1 NaCl), and 11.7 % for D_{12} (0.01 NaCl), suggesting that salt condition was an important factor that affected the adsorption of humic acid. For both CaCl₂ and NaCl, a steep increase in adsorption efficiency was observed when the salt concentration increased from 0 to 0.01 M. Over the concentration range (0.01, 0.1 M), the increase was much slower. This trend is clearly shown in Fig. 4a–c, which plots the adsorption efficiency against the CaCl₂ concentration at pH 5, 7, and 9, respectively. The rationale is that increasing [CaCl₂] reduces the thickness of the electric double layer, and thus reduces the electrostatic repulsion, which promotes the adsorption of humic acid on the NPs. All types of TiO₂ NPs follow a similar sensitivity to the CaCl₂ concentration.

Effect of the cation type on the adsorption efficiency

At the same concentration level, CaCl₂ had higher positive effect on humic acid adsorption than NaCl. Specifically, Tukey–Kramer comparison showed that the effect difference between CaCl₂ and NaCl on zeta potential was estimated to be (56.7, 59.8 %) and (1.0, 4.1 %) at 0.01 and 0.1 M, respectively (Table S3 in Supplementary material). At the same concentration, CaCl₂ has higher ionic strength than NaCl, which induces smaller thickness of the electric double layer. This facilitates the adsorption of humic acid.

Correlation of the adsorption efficiency with the surface charge

The Pearson's correlation between the zeta potential and the adsorption efficiency for humic acid was obtained as 0.797, which indicated that the adsorption efficiency of humic acid was positively proportional to the zeta potential of TiO₂ NPs. The positive correlation between the adsorption efficiency and the zeta potential is graphically illustrated in Fig. 5. This is due to the fact that the humic acid is negatively charged. When the NP surface is negatively charged, the electrostatic repulsion suppresses the adsorption of

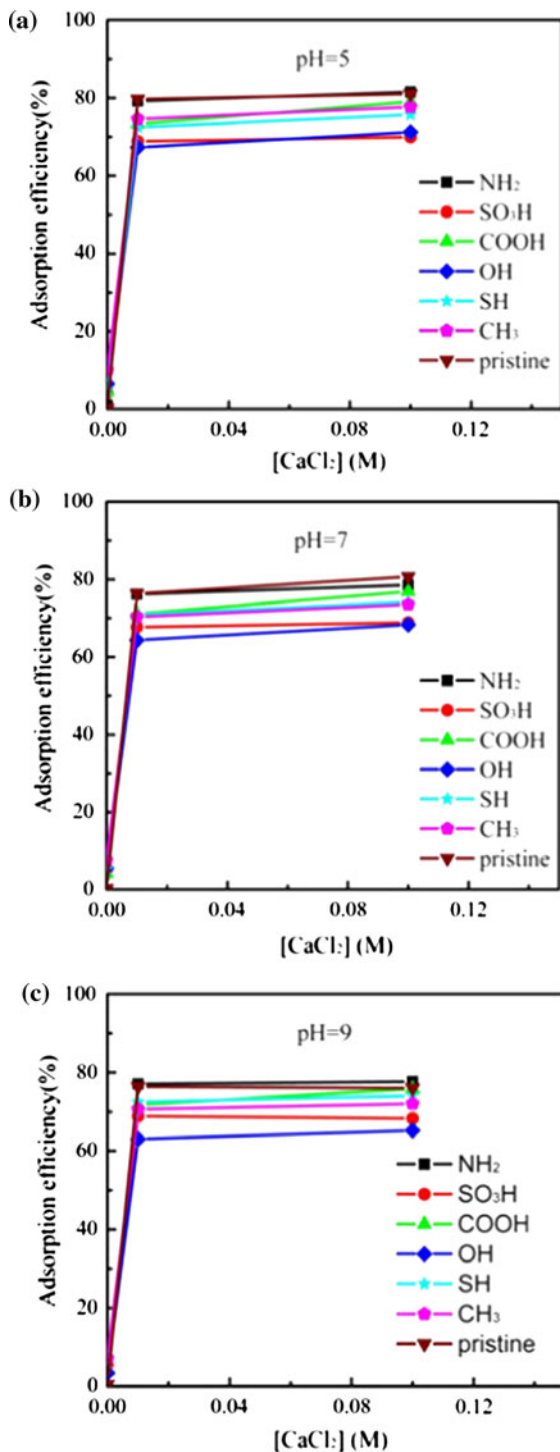


Fig. 4 Adsorption efficiency of various surface-functionalized TiO_2 nanoparticles as a function of CaCl_2 concentration at **a** pH 5, **b** pH 7, and **c** pH 9

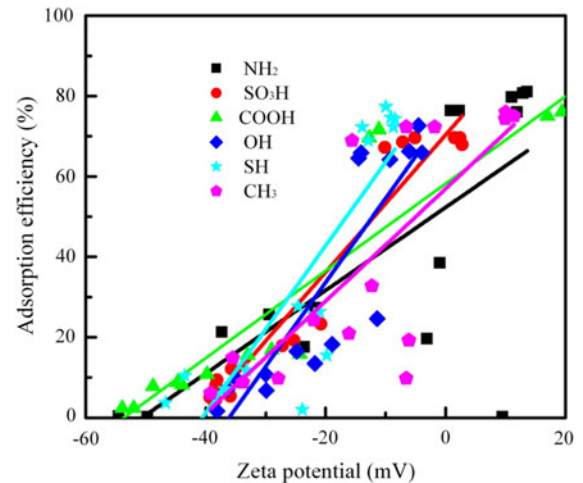


Fig. 5 Correlation of the zeta potential with the adsorption efficiency of humic acid on various surface-functionalized TiO_2 nanoparticles

humic acid. When the NP surface becomes positively charged, the electrostatic attraction takes place, which promotes the adsorption of humic acid on the NP surface. The electrostatic attraction increases with increasing the zeta potential.

Conclusions

The TiO_2 NPs were modified with various terminal groups ($-\text{CH}_3$, $-\text{SH}$, $-\text{OH}$, $-\text{COOH}$, $-\text{SO}_3\text{H}$, and $-\text{NH}_2$). The water quality parameters were adjusted by the changing pH value, the NaCl , and CaCl_2 concentrations. Experimental design was used to determine statistical relationships between a number of dependent and independent variables, and to provide an efficient approach to extract useful information from a complicated system. Results of surface charge, aggregation and adsorption were analyzed by multiple regression models to determine the dominant impact factor on the behaviors of functional NPs.

The zeta potential of NPs decreased with an increase in the pH value, which was ascribed to the deprotonation of surface functional group and the adsorption of hydroxyl group. The zeta potential increased with an increase in the salt concentration at the whole pH range for all the NPs, which was due to the fact that addition of salt increased the ionic strength and thus reduced the

thickness of the electric double layer. Furthermore, the TiO₂ NPs with different functional groups exhibited different zeta potentials that depended on the salt concentration. The zeta potential was in the order of NH₂ > CH₃ > SH (OH, SO₃H) > COOH at a low salt concentration while COOH > NH₂ > SO₃H (CH₃, SH and OH) at a high salt concentration. The zeta potential was significantly higher in the CaCl₂ solution than that in the NaCl solution.

At a low salt concentration, the hydrodynamic size was little affected by the pH value. At a high salt concentration, the hydrodynamic size increased with increasing the pH value. Addition of CaCl₂ into the aqueous solution significantly increased the hydrodynamic size but further increasing the CaCl₂ concentration caused different changes in the hydrodynamic size for different functional group-modified NPs. Significant two-factor interactions between NH₂ group and 0.1 M CaCl₂, and between COOH group and 0.1 M CaCl₂ were observed.

There was a negative correlation between the hydrodynamic size and the absolute value of zeta potential while a positive correlation between the hydrodynamic size and the ionic strength, which indicated that the DLVO mechanism played a significant role. The NH₂-TiO₂ and the COOH-TiO₂ NPs had larger hydrodynamic size than the other types of NPs at the same CaCl₂ concentration and at the same pH value because the amine and the carboxyl groups strongly tended to form a chelate complex with Ca²⁺.

The adsorption efficiency of humic acid decreased with an increase in the pH value, whereas increased with an increase in the salt concentration. The adsorption efficiency of humic acid in CaCl₂ solution was higher than that in the NaCl solution and positively correlated with the zeta potential.

Acknowledgments This work was financially supported by the NSF Grants (CBET-0834233 and CBET-1065931). The facilities and resources used in this work were partially supported by the NSF Grant (EPS 1003907) with the matching funds from the West Virginia University Research Corporation and the West Virginia EPSCoR Office. The use of WVU Shared Facility is greatly appreciated.

References

- Cano-Serrano E, Blanco-Brieva G et al (2003) Acid-functionalized amorphous silica by chemical grafting-quantitative oxidation of thiol groups. *Langmuir* 19:7621–7627
- Chen G, Liu X et al (2012) Distinct effects of humic acid on transport and retention of TiO₂ rutile nanoparticles in saturated sand columns. *Environ Sci Technol* 46:7142–7150
- Derjaguin B, Landau L et al (1941) Theory of the stability of strongly charged lyophobic sols and of the adhesion of strongly charged particles in solutions of electrolytes. *Acta Physicochim* 14:633–662
- Domingos RF, Tufenkji N et al (2009) Aggregation of titanium dioxide nanoparticles: role of a fulvic acid. *Environ Sci Technol* 43:1282–1286
- Duan DM, Wu NQ et al (2001) Length scale effect on mechanical behavior due to strain gradient plasticity. *Mater Sci Eng A* 303:241–249
- Epling GA, Lin C (2002) Investigation of retardation effects on the titanium dioxide photodegradation system. *Chemosphere* 46:937–944
- French RA, Jacobson AR et al (2009) Influence of ionic strength, pH, and cation valence on aggregation kinetics of titanium dioxide nanoparticles. *Environ Sci Technol* 43:1354–1359
- Fumiaki A, Taikei Y et al (2010) Highly active titania photocatalyst particles of controlled crystal phase, size, and polyhedral shapes. *Top Catal* 53:455–461
- Gu YY, Yeung AT et al (2009) Effects of chelating agents on zeta potential of cadmium-contaminated natural clay. *Sep Sci Technol* 44:2203–2222
- Hamilton RF, Wu N et al (2009) Particle length-dependent titanium dioxide nanomaterials toxicity and bioactivity. *Part Fibre Toxicol* 6:35
- Hyung H, Kim JH (2008) Natural organic matter (NOM) adsorption to multi-walled carbon nanotubes: effect of NOM characteristics and water quality parameters. *Environ Sci Technol* 42:4416–4421
- Hyung H, Fortner JD et al (2007) Natural organic matter stabilizes carbon nanotubes in the aqueous phase. *Environ Sci Technol* 41:179–184
- Keller AA, Wang H et al (2010) Stability and aggregation of metal oxide nanoparticles in natural aqueous matrices. *Environ Sci Technol* 44:1962–1967
- Kim Y, Johnson RC et al (2001) Gold nanoparticle-based sensing of “spectroscopically silent” heavy metal ions. *Nano Lett* 1:165–167
- Lee PF, Sum DD et al (2007) Adsorption and photodegradation of humic acids by nano-structured TiO₂ for water treatment. *J Adv Oxid Technol* 10:72–78
- Li M, Zhou S, Zhang et al (2008a) One-step solvothermal preparation of TiO₂/C composites and their visible-light photocatalytic activities. *Appl Surf Sci* 254:3762–3766
- Li M, Tang P et al (2008b) High efficient surface-complex-assisted photodegradation of phenolic compounds in single anatase titania under visible-light. *Colloid Surf A Physicochem Eng Aspects* 318:285–290
- Li M, Hong Z et al (2008c) Synergistic effect of two surface complexes in enhancing visible-light photocatalytic activity of titanium dioxide. *Mater Res Bull* 43:2179–2186
- Li H, Lai F et al (2009) Analysis of responsive characteristics of ionic-strength-sensitive hydrogel with consideration of effect of equilibrium constant by a chemo-electro-mechanical model. *Langmuir* 25:13142–13150
- Li M, Cushing SK, Wang Q, Shi X, Hornak LA, Hong Z, Wu NQ (2011) Size-dependent energy transfer between CdSe/

- ZnS quantum dots and gold nanoparticles. *J Phys Chem Lett* 2:2125–2129
- Liu X, Chen G et al (2011) Effects of material properties on sedimentation and aggregation of titanium dioxide nanoparticles of anatase and rutile in the aqueous phase. *J Colloid Interf Sci* 363:84–91
- Magrez A, Horváth L et al (2009) Cellular toxicity of TiO₂-based nanofilaments. *ACS Nano* 3:2274–2280
- Montgomery DC (2012) Design and analysis of experiments, 8th edn. Wiley-Interscience, Chichester
- Morrison ID, Ross S (2002) Colloidal dispersions: suspensions, emulsions, and foams. Wiley-Interscience, New York
- Mueller NC, Nowack B (2008) Exposure modeling of engineered nanoparticles in the environment. *Environ Sci Technol* 42:4447–4453
- Ofir E, Oren Y et al (2007) Electroflocculation: the effect of zeta potential on particle size. *Desalination* 204:33–38
- Palma RD, Peeters S et al (2007) Silane ligand exchange to make hydrophobic superparamagnetic nanoparticles water-dispersible. *Chem Mater* 19:1821–1831
- Sharma VK (2009) Aggregation and toxicity of titanium dioxide nanoparticles in aquatic environment—a review. *J Environ Sci Health A* 44:1485–1495
- Smith B, Wepasnick K et al (2009) Influence of surface oxides on the colloidal stability of multi-walled carbon nanotubes: a structure–property relationship. *Langmuir* 25:9767–9776
- Solovitch N, Labille J et al (2010) Concurrent aggregation and deposition of TiO₂ nanoparticles in a sandy porous media. *Environ Sci Technol* 44:4897–4902
- Tafen D, Wang J et al (2009) Visible light photocatalytic activity in nitrogen-doped TiO₂ nanobelts. *Appl Phys Lett* 94:093101
- Tamhane AC, Dunlop DD (2000) Statistics and data analysis from elementary to intermediate. Prentice Hall, Upper Saddle River
- Tan GL, Hömmerich U et al (2003) Synthesis and optical characterization of CdTe nanocrystals prepared by ball milling process. *Scr Mater* 48:1469–1474
- Verwey EJW, Overbeek JTG (1948) Theory of the stability of lyophobic colloids. Elsevier, Amsterdam
- Wang P, Shi Q et al (2008) Enhanced environmental mobility of carbon nanotubes in the presence of humic acid and their removal from aqueous solution. *Small* 4:2166–2170
- Wang J, Tafen DN et al (2009) Origin of the photocatalytic activity of nitrogen-doped TiO₂ nanobelts. *J Am Chem Soc* 131:12290–12297
- Wang D, Zhao H et al (2010) Tuning the charge transfer property of PbS-quantum dot/TiO₂-nanobelt nano hybrids via quantum confinement. *J Phys Chem Lett* 7:1030–1035
- Wu NQ, Zhao M et al (2005) Porous CuO–ZnO nanocomposite for sensing electrode of high-temperature CO solid-state electrochemical sensor. *Nanotechnology* 16:2878–2881
- Wu NQ, Wang J et al (2010) Shape-enhanced photocatalytic activity of single-crystalline anatase TiO₂ (101) nanobelts. *J Am Chem Soc* 132:6679–6685
- Yang M, Wang J et al (2008) A lactate electrochemical biosensor with a titanate nanotube as direct electron transfer promoter. *Nanotechnology* 19:075502
- Yang K, Li D et al (2009) Interactions of humic acid with nanosized inorganic oxides. *Langmuir* 25:3571–3576
- Zhang S, Shao T et al (2009) The impacts of aggregation and surface chemistry of carbon nanotubes on the adsorption of synthetic organic compounds. *Environ Sci Technol* 43:5719–5725
- Zhang Q, Sun T et al (2010) Tuning the shape and thermoelectric property of PbTe nanocrystals by bismuth doping. *Nanoscale* 2:1256–1259
- Zhu ZJ, Carboni R et al (2010) Surface properties dictate uptake, distribution, excretion, and toxicity of nanoparticles in fish. *Small* 6:2261–2265